

Special grain boundaries based on local symmetries

L. A. Bendersky · J. W. Cahn

Received: 11 May 2006 / Accepted: 26 June 2006 / Published online: 7 November 2006
© Springer Science+Business Media, LLC 2006

Abstract We propose that, in large unit cell structures, the operation of local symmetries rather than a coincidence site lattice (CSL), is important for the creation of special, low energy, grain and twin boundaries. We illustrate this with a Dürer tiling, and its monoclinic realization, as well as with crystals with large icosahedral motifs.

Introduction

Thanks to the pioneering work of David Brandon [1, 2] and many others [3, 4], we know that special grain boundaries are likely to occur when the two abutting crystal with face- or body-centered cubic structures are oriented to form a three-dimensional coincidence site lattice (CSL). The CSL concept began with Friedel's work on twinning [5]. He proposed that twins be defined by a shared common lattice, a twin lattice. When the grain boundaries or twin boundaries thread through common lattice sites, any atoms on those coinciding lattices sites fit into both grains, and this possibly results in low energy and other special properties. This simple idea has been widely invoked, but it ignores many factors, and overemphasizes some.

CSLs (and twin lattices, which for convenience we will subsume under CSLs) are characterized by a single positive integer, Σ , which is the ratio of the volumes of the unit cells in the CSL and the lattice of either crystal, respectively. Therefore, unless the CSL has three-dimensional periodicity, Σ is not defined. This requirement of three-dimensional periodicity specifies a set of exact rotations and, for each non-cubic crystal system, a set of Friedel twinning "laws" [5–7], which place additional conditions on the lattice parameter ratios and the cell angles of the unit cells.¹ Grain and twin boundaries with deviations from these conditions on the rotation and on the unit cell parameters are commonly observed and this has led to an assumption that many properties are continuous functions of the unit cell parameters through the exact conditions. This in turn has created a need to specify how much deviation can be tolerated for a bicrystal and its grain boundary to have approximately the special properties associated with a CSL.

The principal idea in this paper is that the properties of twin or grain boundary should depend only on the local atomic arrangement near it. Invoking the CSLs guarantees that atoms on the coinciding sites fit into both crystals, but regions of poor fit fall between the sites. Should we be looking for other criteria? Consider the following:

- (1) Why should the few coincidence points have such an important effect, when most of the atoms near a grain or twin boundary are not on such points? As Σ increases, its effect must decrease, while it

L. A. Bendersky (✉) · J. W. Cahn
Materials Science and Engineering Laboratory, National
Institute of Standards and Technology, 100 Bureau Dr.,
Bldg 223, A147, Gaithersburg, MD 20899-8555, USA
e-mail: leonid.bendersky@nist.gov

¹ These "laws" require certain ratios to be rational fractions. For Σ to be small these fractions must be ratios of small integers.

persists for near-CSL conditions where Σ is infinite in a strict definition.

- (2) In a three-dimensional CSL, why should coincidence points distant from a grain or twin boundary have any effect on it?
- (3) For non-cubic crystals not satisfying the twinning “laws” we can create a symmetric tilt boundary on any rational plane with the same kind of fit along it as if there had been a CSL.
- (4) Grain boundaries are characterized by five angular variables (two if they are between two-dimensional crystals). The CSL is specified by the three angles which give the relative orientation of the two crystals; missing are the two other angles which specify the orientation of the tangent or normal to the boundary. CSLs, even between cubic crystals, are never cubic, and often have large axial ratios. The density of CSL sites is strongly dependent on the orientation of every rational plane through lattice sites. Is there a correspondence between the orientation dependence of this density and the energy of the boundary?
- (5) Crystal lattices, and the diffraction intensity from the crystals, can be considered invariant to any translations, but the atomic structures at the boundary depend on the relative translation of the crystals along and normal to the boundary. Lattices can be shifted to give the highest density of coincidences on a boundary. Crystals can be shifted to give the best atom fit. Is there any connection between these shifts?

We will address some of these questions with a boundary in a two-dimensional tiling first displayed by Albrecht Dürer, and then by TEM projections of grain boundaries between three-dimensional $\text{Al}_{13}\text{Fe}_4$ crystals, a polycrystalline aggregate of cubic- α - $\text{Al}_9(\text{Mn}, \text{Fe})_2\text{Si}_2$ and a collection of examples from our work and the literature.

A two-dimensional example: the Dürer tiling

We begin with a two-dimensional rectangular tiling structure, Fig. 1a, originally drawn by Dürer and published in 1525 in *A Manual of Measurements of Lines, Areas, and Solids by Means of Compass and Ruler* [8]. In each centered rectangular unit cell of this periodic structure with plane group $c2mm$, Fig. 1b, there are two-fold axes, mirrors shown as solid lines, and glide mirror shown as dashed lines. The centered unit cell has four pentagons in two orientations and two skinny rhombuses.

For there to be a CSL the ratio b^2/a^2 has to be a rational fraction with small integers [5, 6]. If we let the length of the sides of the regular pentagons be 1, the long side of the unit cell $a = 4\sin(\pi/5) + 2\sin(2\pi/5) = 4.979\dots$, and the short side $b = 1 + 2\cos(\pi/5) = \tau = 1.618034$, where $\tau = (1 + \sqrt{5})/2$ is the golden mean. Then $b^2/a^2 = 9.472\dots$. Since this is irrational there can be no two-dimensional CSL.

With these tiles Dürer displayed a ten-grain structure with a perfect match of all tiles throughout, within the grains and across the grain boundaries, with no distortions or changes in coordination number (Fig. 1c). Clearly these would be good interfaces. The grain boundaries interrupt the translational symmetry

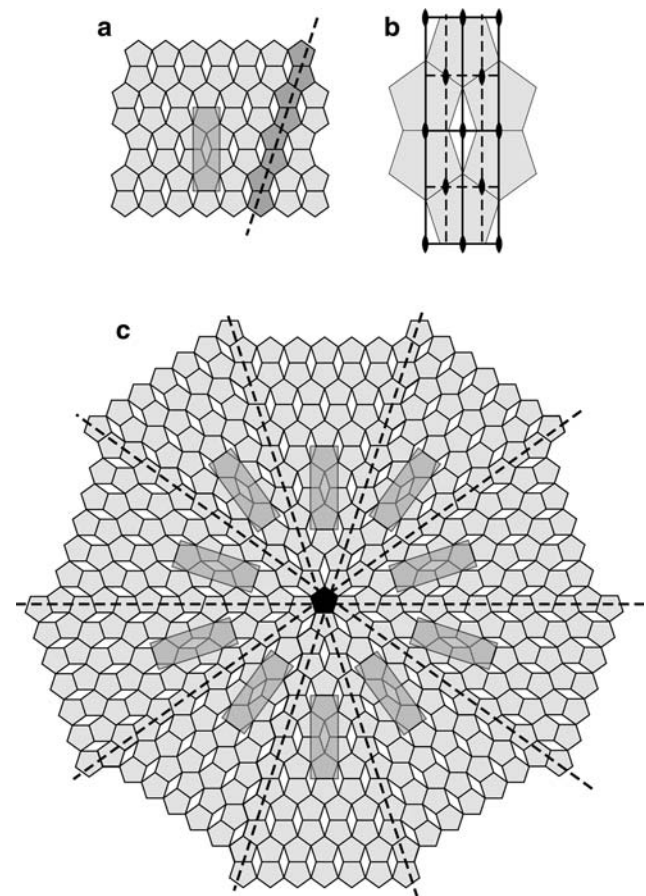


Fig. 1 Dürer's tiling of pentagons and rhombuses. **(a)** The periodic tiling with a centered rectangular unit cell outlined, and a local glide mirror (11) line, bisecting two of the pentagon edges, indicated by a dashed line. **(b)** The $c2mm$ unit cell and its symmetry elements [6]. The local glide mirror line contains the two-fold axes. **(c)** Ten wedge-shaped crystals arranged by Dürer in five orientations $\pi/5$ rad or 36° apart. Note that all pentagons are in one of just two orientations, that each grain boundary is along a glide mirror line, and that each entire pentagon along that line fits into both crystals

and produce ten lattices, each rotated from its neighbors by $\phi = 2 \arctan a/b = \pi/5$ rad (or 36°). All the pentagons in every crystal have either of these same two orientations. Each $\pi/5$ rotation converts the two pentagons into each other.

Each grain boundary is a straight tilt boundary with a displacement along the (1 1) for both crystals; because of this displacement the boundary is along a glide mirror line of each bi-crystal in Fig. 1c, as indicated by the dashed lines.

Since “reflection” is another definition of twins, Fig. 1c shows a ten-fold twin, even though the Friedel twinning laws are not met. Each pair of adjacent grains form a perfect glide reflection twin.

The CSL rules place the boundary along a high density of CSL points or the O-lattice points, or along an O-line [3]; they all fail in this example. The translation vector of this centered unit cell and the periodicity along the boundary are both $(1/2)\langle 11 \rangle$. Since the glide component of the reflection is $(1/4)\langle 11 \rangle$, this glide distance has the largest possible difference from the coincidence along the boundary, which assures that there are no O-lattice points or O-lines in its vicinity. There are O-lattice lines parallel to the boundary, spaced periodically $(a/4)\sqrt{(a^2 + b^2)} = 6.225\dots$, which is incommensurate with the spacing of (1, 1) lattice lines, and symmetrically arrayed about the boundary, and as far away as possible from it [9].

A one-dimensional set of coincidence points can be created along any grain boundary by shifting the lattices. However, if the origins of the lattice are chosen to be at either of the Wyckoff sites with 2mm symmetries, there are no coinciding lattice points anywhere, and the boundary is along a line with the largest separation anywhere between lattice points in the two structures. If one accepts as coincidences point which are separated by less than some ϵ there will be a quasiperiodic CSL. This quasilattice is symmetric about the boundary, but again with no points near it.

The reason for the good fit along the boundary is not because there is a CSL or an O-line; it originates in a local symmetry which is not a symmetry operation of the structure. In the Dürer tiling this is a *local* glide mirror along the (1 1), which leaves the pentagons along it invariant, as shown by the dashed line in Fig. 1a, but because it is not a symmetry operation of the periodic tiling, the operation of this local glide mirror creates the grain boundary with the excellent fit.

The five-fold rotation of individual pentagons is an alternate local symmetry, which is not a symmetry operation of the crystal, to consider. While this rotation of a structural motif predicts the correct tilt

angle, its range of good fit does not extend beyond the pentagon and one of its neighbors.

Experimental examples

Monoclinic $\text{Al}_{13}\text{Fe}_4$

Twinning with an apparent non-crystallographic ten-fold rotation axis was observed for crystals of a monoclinic Al_3Fe (or $\text{Al}_{13}\text{Fe}_4$) phase (mC102, $C2/m$) with β near $(3/5)\pi$ (or 108°). This phase is stable and occurs in a number of Al-transition metals systems, e.g., Al-Co, Al-Ru and Al-Rh [10]. Its structure was determined and analyzed by Black [11] and is shown in Fig. 2a projected along the [010] direction.

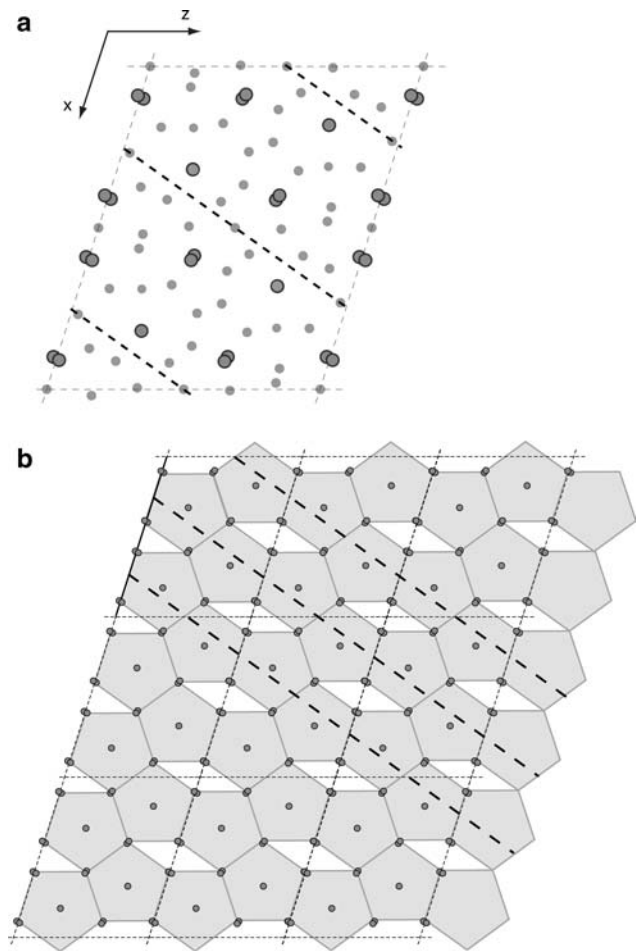


Fig. 2 The crystal structure of monoclinic $\text{Al}_{13}\text{Fe}_4$, $C2/m$. **(a)** A unit cell projected along [010], showing the approximate local glide mirrors as dashed lines. Fe atoms are darker and larger. **(b)** The projection of the crystal structure with only the Fe atoms shown in a Dürer tiling (shaded, compare with Fig. 1a) and unit cells (dotted lines). The corners are marked by pairs of Fe. The approximate local glide mirrors which go through a set of two-fold inversion axes [6] accurately bisect the pentagon edges

To emphasize that the projected structure can be tiled approximately as the Dürer tiling, only the projected Fe atoms are shown in Fig. 2b. There are columns of Fe atoms, two per unit cell, at the corners of the tiling, and an Fe at the center of the pentagons. The tiling of pentagons is indeed the same as the periodic tiling of Dürer, Fig. 1a. Therefore the same special boundaries as in Dürer's pentagonal twins are not unexpected for $\text{Al}_{13}\text{Fe}_4$.

To see if the planes, which are indicated by the dashed lines, are approximate local glide planes, we have to look at how well the atoms superimpose after a glide reflection. Unlike perfect superposition for the entire row of pentagons in the Dürer tiling after the glide reflection, we can't expect perfection. Ignoring the direction of the projection, the superposition is good for the atoms along the line itself and for most of the atoms within the row of pentagons. As in the Dürer tiling the fit becomes less good further away, but that is of little consequence for a glide reflection twin boundary along this plane.

Indeed, in rapidly solidification conditions out in Al-rich alloys, the primary $\text{Al}_{13}\text{Fe}_4$ phase grows often in a form of star-like twinned crystals. Beautiful examples of these twins with a 10-point star morphology were reported by Louis et al. [12] for an Al-Fe alloy, and Fung et al. [13] and Steeds et al. [14] have reported examples of the $\text{Al}_{13}\text{Fe}_4$ microtwins coexisting with the decagonal quasicrystal. Figure 3a shows a high resolution image of one of such aggregates which we observed occasionally in a melt spun $\text{Al}_{70}\text{Fe}_{13}\text{Si}_{17}$ alloy. The image is obtained with the [010] direction parallel to an electron beam.

The upper part of the image shows a fan of crystals. Rotation between adjacent crystals was measured to be 36° , and therefore the crystals are related to each other by ten-fold rotations. According to the tiling representation of the image, Fig. 1c, the rotated crystals are aggregates with invariant orientations of two mirror-related pentagons, and good overlap of structural units. The boundary, shown as a tiling in Fig. 3b, can be considered as a (201) glide mirror plane of the monoclinic lattice, or a (101) if we approximate it by a orthorhombic lattice. The described twinning is similar to multiple twinning observed in the τ^2 -inflated $\text{Al}_{13}\text{Co}_4$ [15] (201) glide twins. Again, an approximate local glide reflection symmetry permits the formation of a well fitting twin boundary.

The bottom part of the image in Fig. 3a has a crystal with planar defects of varying thickness, which are parallel to (001). Thicker defects are recognized as twins produced by (001) mirror reflection—a twinning of a monoclinic lattice, which can not be discerned in

the two-dimensional tiling, and which again does not change the orientation of pentagons. The (001) and (100) twinning was suggested by Black [11], with a structural model involving the (001) glide twinning plane. The (001) and (100) twins were found in the τ^2 -inflated $\text{Al}_{13}\text{Co}_4$ phase by means of electron diffraction [16].

α -cubic Al-Mn-Fe-Si

We studied the effect of the substitution of Mn by Fe on microstructure of $\text{Al}_{(91-93)}(\text{Mn,Fe})_{(5-7)}\text{Si}_2$ and $\text{Al}_{75}(\text{Mn, Fe})_{15}\text{Si}_{10}$ rapidly solidified alloys [17, 18]. The alloys were prepared by different methods, including melt spinning, surface e-beam melting and powder atomization. Typically, the microstructures consist of primary solidified nodules surrounded by a duplex structure. Examples of the microstructures observed for high-Al $\text{Al}_{(91-93)}(\text{Mn,Fe})_{(5-7)}\text{Si}_2$ are shown in Fig. 4. Although morphologically the struc-

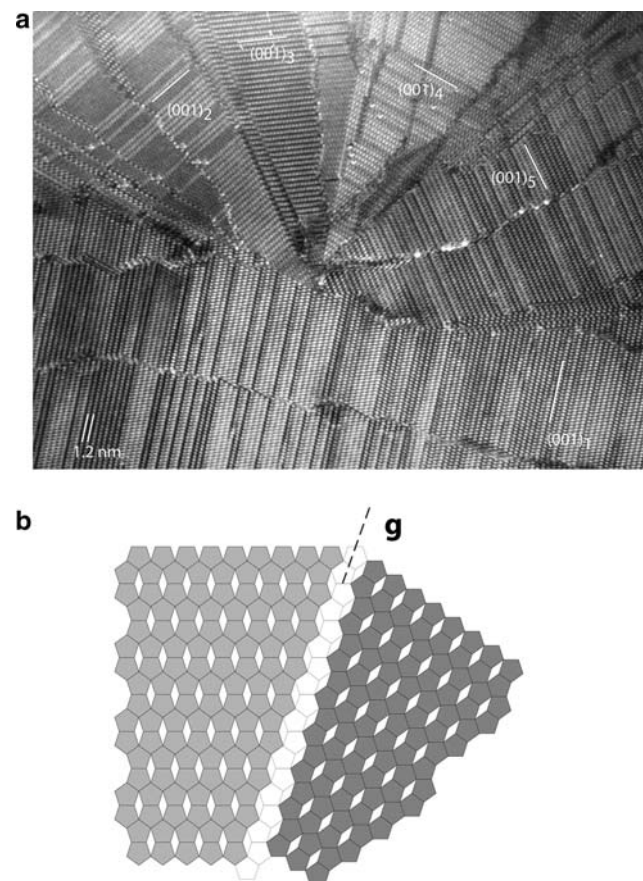


Fig. 3 An aggregate in a melt spun $\text{Al}_{70}\text{Fe}_{13}\text{Si}_{17}$ alloy. **(a)** A high-resolution TEM image with [010] parallel to the beam. Compare with Fig. 1c. **(b)** The analog of the twins in the Dürer tiling. The twin boundary is a the glide mirror plane of the bicrystal

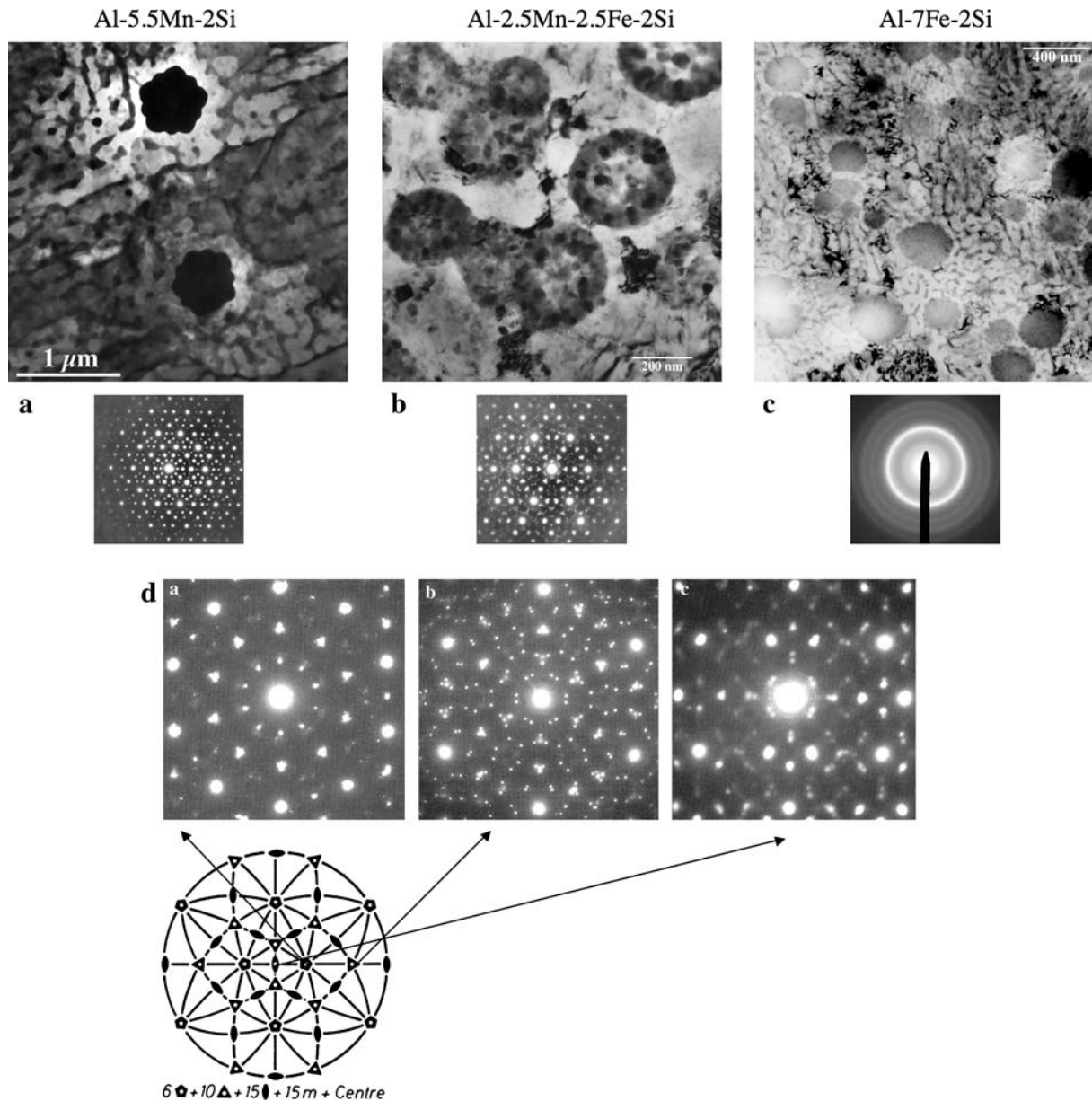


Fig. 4 The effect of substituting Fe for Mn is a series of Al–Mn–Fe–Si alloys. **(a)** Diffraction from alloys with no Fe shows nodules of the icosahedral phase. **(b)** With Fe/Mn = 1, a single nodule of a polycrystalline aggregate shows major SAED patterns similar to that of the icosahedral phase. However, instead of reflections of the icosahedral phase, these are clusters

of spots belonging to five variants of the cubic approximant periodic phase $Al_9(Fe, Mn)_2Si_2$, $a = 1.26$ nm, $cI144$, $Im\bar{3}$. **(c)** The alloy with no Mn shows nodules with a glassy diffraction pattern. **(d)** Rotating the aggregate in **(b)** shows that it accurately mimics icosahedral symmetry

tures look similar, there a is profound effect of substituting Fe for Mn. As evident from the diffraction patterns, the nodules have significantly different structures: alloys containing no-Fe have an icosahedral phase (Fig. 4a), alloys containing no Mn are glassy (Fig. 4c), and the alloys with Fe/Mn = 1 give an unusual polycrystalline structure (Fig. 4b). The diffraction pattern of this polycrystalline structure resembles that of the icosahedral phase, namely having average

symmetries and angular relationship of the five-, three- and two-fold axes, Fig. 4d, but analysis of the patterns determined that the polycrystalline structure consists of small grains of the cubic α - $Al_9(Mn, Fe)_2Si_2$ phase (space group symmetry $Im\bar{3}$, $a = 1.26$ nm [19–23]). Because there are only five orientational variants of the grains, the composite diffraction pattern of hundreds of grains in one nodule appears as that of a single crystal. The orientations of the variants is such that the

fifteen two-fold axes of an icosahedron are grouped into five sets of mutually orthogonal triplets; the axes of each cubic crystal are parallel to one of the orthogonal two-fold triplets. If one set is along $\langle 100 \rangle$'s, the 12 other two-fold axes are along $\langle 1, \tau, (1 + \tau) \rangle$ axes. Thus, e.g., the triplet $[(1 + \tau), -1, \tau]$, $[-1, \tau, (1 + \tau)]$, and $[\tau, (1 + \tau), -1]$ defines the orientation of another variant. (The algebraic property of Golden Mean, $\tau^2 = 1 + \tau$, is used to show orthogonality of the axes.) The misorientations between any two grains are the same irrational rotations generated by the operation of icosahedral symmetry elements.

Confirmation for the non-crystallographic orientation relationship was also found in high-resolution structural TEM images. An example in Fig. 5 shows a grain boundary between two cubic crystals of the α -Al–Mn–Fe–Si phase, both oriented with a $[111]$ axis parallel to the electron beam. The 110 planes are rotated to each other 15.6° or 44.4° (exact icosahedral

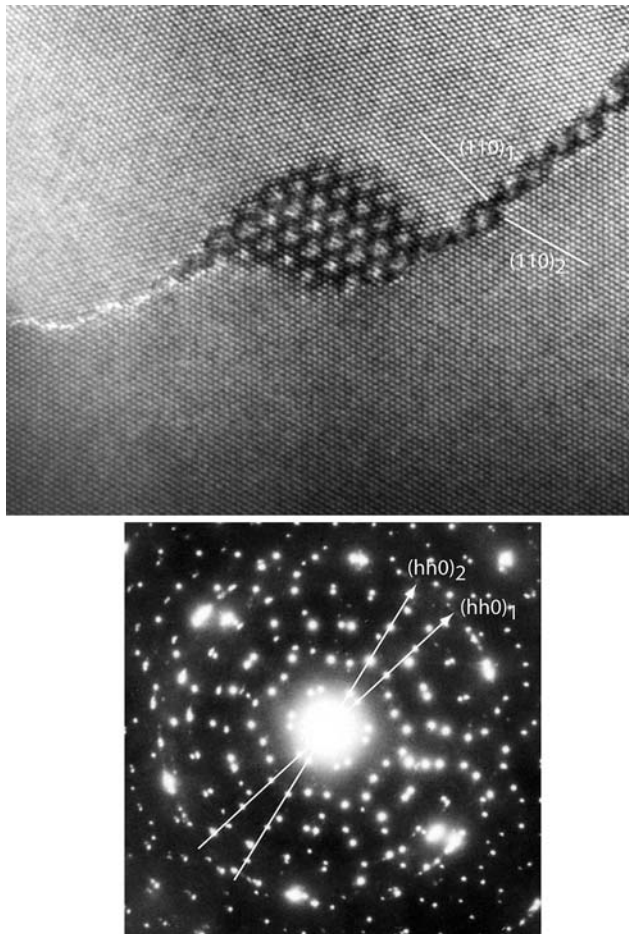


Fig. 5 A grain boundary between two α -cubic phase crystals, oriented with their common $[111]$ tilt axis parallel to the electron beam. The $\{110\}$ are rotated by 15.6° or 44.4° (the exact icosahedral symmetry gives 44.48°) ($\arcsin[\sqrt{3}/4] = 44.48^\circ$). There are no $[111]$ CSL rotations close to the measured 44.4°

symmetry gives 44.48°) ($\arcsin[\sqrt{3}/4] = 44.48^\circ$). There are no CSL rotations about $[111]$ which are close to the measured 44.4° . Even though the crystals are cubic, there is no low Σ CSL for the observed rotations.

This cubic α -Al₉(Mn,Fe)₂Si₂ structure is not a good candidate for special boundaries based on the coincidence of at most two atoms out of 144 atoms in a unit cell, bearing in mind that it could be none, since the positions with cubic symmetry are unoccupied. The structure is an approximant [19] of the icosahedral phase considered as a bcc packing of multishell clusters (motifs) of near-icosahedral symmetry. Connectivity of the clusters in a cell through overlap of outer shells [20] along the three-fold $\langle 111 \rangle$ directions maintains the long-range orientational order in both this and the icosahedral phase.

The experimental results imply that the approximately icosahedral motifs of the cubic phase continue to pack across these grain boundaries with no detectable change in orientation. Even though the lattices rotate, the motifs do not rotate and retain the same orientation in all crystals and in the grain boundaries within one polycrystalline nodule. The changes in orientation of the cubic lattices were found to be non-crystallographic symmetry operation of the icosahedra, five-fold rotations along irrational axes of the cubic system, which kept all the atoms in the motifs along the grain boundary intact, and their number can be much greater than any CSL of this large unit cell. These results support a need for an enlarged criterion for the existence of special grain boundaries.

Other examples from the literature

Some additional examples of the same phenomena of crystalline aggregates with invariant orientation of motif can be found in the literature. Such a parallelism of motifs has been reported in microcrystalline structures displaying “apparent” icosahedral symmetry in a Ni–Ti alloy [24] and “apparent” decagonal symmetry in V–Ni–Si [25] and Al–Fe–Ce [14] alloys. In these observations the crystals were so small that they were called, respectively, “local translational order in a quasicrystal” and “microdomains”. An example of icosahedral twinning of a monoclinic Al₄₅Cr₇ phase was found by Zhang et al. [26]. In that case the structural motif is a simple 13 atoms icosahedron which remains orientationally invariant throughout the observed crystalline aggregate. With that condition 30 orientation variants of the monoclinic phase are possible. In a study of an octagonal quasicrystal in Cr–Ni–Si, polycrystals that were called “ 45° twins” ($\pi/4$) and “microtwins of the beta-manganese

structure” were observed [27, 28]. It is obvious from the diffraction patterns that such a rotation does not lead to a twin lattice. Therefore, this is an eight-fold example of the motif invariant orientation relationship. But even in the case of merohedral twinning in pyrite, Donnay et al. [29] concluded that the main feature of that twinning is an invariance of the lattice complex occupied by Fe.

Discussion

The generalization that we draw from these examples is that the operation of local symmetries of crystal structures, which are not symmetry operations of the entire crystals, can create defects, in these examples interfaces, in which there is little or no atomic mismatch extending over several atomic layers. This is in contrast to an interface in a CSL for which there is a modulation of distortions between the points of exact fit.

Dürer’s geometrical example with a centered rectangular structure illustrates that it is possible to have an interface consisting of a continuous chain of pentagons which fit perfectly into either crystal. There is no distortion anywhere; every feature fits into one or both of the crystals. A local glide mirror along (11) was present in each tiling crystal as a local approximate symmetry element which extends to cover just a $\langle 11 \rangle$ periodic chain of pentagons. In the twinned bicrystal this periodic chain is converted into a perfect glide mirror along the twin interface; the crystals are in reflection twin orientations to each other, however, with a glide component.

Because b^2/a^2 is irrational there can be no two-dimensional CSL. The center of the interface does not occur at a line in which there is coincidence; it is instead where the deviation from coincidence is a maximum, at half of the interface periodicity. This interface with this excellent fit is not one that would be chosen with any of the CSL criteria.

The experimental examples show an example of an approximate local glide mirror plane and several examples of local icosahedra, a non-crystallographic motif, and an eight-fold motif. The $\text{Al}_{13}\text{Fe}_4$ in projection mimics the local glide mirror of the Dürer tiling quite well. In the crystals with local icosahedral motifs, icosahedral rotations will leave the motifs unrotated and only slightly distorted at the grain boundaries, but crystal axes will rotate. Because the $\alpha\text{-Al}_9(\text{Mn, Fe})_2\text{Si}_2$ is cubic, it can have rotations that give CSL, but such rotations would greatly distort the large icosahedral motifs in the region of the grain boundary, and are likely to be of high energy.

In each of these cases there are local symmetries that are not symmetries of the individual crystals. These can be crystallographic, as in the case of the glide mirror in Al–Fe and the four-fold in merohedral pyrite, or non-crystallographic, five-fold in the case of the cubic $\alpha\text{-Al-Fe-Mn-Si}$ and eight-fold in Cr–Ni–Si.

The rotations to consider for special low energy grain boundaries are those compatible with the motifs but not with the crystal structure. One way of reconciling this view with the CSL methods is to recognize that a single metallic atom is a motif with the highest non-crystallographic symmetry of the holohedral infinite rotation group, compatible with any rotation, provided the angular arrangement of neighbors is of lesser importance. Then CSL rotations have an energetic advantage of increasing the density of well-fitting atoms. But whenever the atom becomes part of a large motif, the CSL rotations are unlikely to be compatible with it. Then rotations which will leave the motif unaffected need to be considered, and the problem becomes one of finding interface geometries which raise the density of these motifs.

This creates an emphasis on details of crystal structures, not just on the ratios of lattice parameters and unit cell angles, but also on the numbers in the Wyckoff positions. That $\beta \approx 108^\circ$ is important for the $\pi/5$ twins. In a cubic structure with an $m\bar{3}$ point group $m\bar{3}m$, there are 12m positions of the type 0, y, z. For those positions to form a regular icosahedron, the ratio of x to y has to be near τ or $1/\tau$. For the Al position in Al_{12}Re , for example, $x/y = 1.638$ [10].

The rigid conditions for twin lattices seem to have fallen out of favor among crystallographers. For hexagonal and tetragonal alloys in which the c^2/a^2 ratio varies with composition, there seems to be no special twinning effects when it becomes rational with small integers. The twinning “laws” are not mentioned in the latest edition of the International Tables for crystallography [30]. Will there be a similar shift in emphasis for grain boundaries?

References

1. Brandon DG, Ralph B, Ranganathan S, Wald MS (1964) Acta Metall 12:813
2. Brandon DG (1966) Acta Metall 14:1497
3. Bollmann W (1982) Crystal defects and crystalline interfaces. Springer, New York, p 143ff
4. Sutton AP, Balluffi RW (1995) Interfaces in crystalline materials. Clarendon, Oxford
5. Friedel G (1964) Leçons de cristallographie Paris, 1926, 2nd edn. Librairie Sci. A. Blanchard, Paris
6. Donnay JDH, Donnay G (1985) International tables of X-ray crystallography. Reidel, Dordrecht, V. 2, Sect 3.1.9, p 104

7. Grimmer H, Nespolo M (2006) *Z Kristallogr* 221:28
8. Dürer A (1977) *A manual of measurement of lines, areas and solids by means of compass and ruler 1525* (facsimile Edition, translated with commentary by WL Strauss). Abaris Books, New York
9. Hagege S (1991) *Acta Crystall A* 47:119
10. Villars P, Calvert LD (1991) *Pearson's handbook of crystallographic data for intermetallic phases*, 2nd edn. ASM International)
11. Black PJ (1955) *Acta Crystall* 8:43
12. Louis ER, Mora L, Pastor L (1980) *Metal Sci* 14:591
13. Fung KK, Zou XD, Yang CY (1987) *Phil Mag Lett* 55:27
14. Steeds JW, Ayer R, Lin YP, Vincent R (1986) *J de Physique Colloque C3* 47:437
15. Ma XL, Kuo KH (1992) *Metall Mater Trans* 23A:1121
16. Ma XL, Kuo KH (1995) *Metall Mater Trans* 26A:757
17. Bendersky LA, Ridder SD, Biancaniello FS, Shaprio AJ (1991) *J Mater Sci Eng* A134:1098
18. Bendersky LA, Cahn JW, Gratias D (1989) *Philos Mag B* 60:837
19. Elser V, Henley CH (1985) *Phys Rev Lett* 55:2883
20. Fowler HA, Mozer B Sims J (1988) *Phys Rev B* 37:3906
21. Cooper M, Robinson K (1966) *Acta Crystall* 20:614
22. Cooper M (1967) *Acta Crystall* 23:1106
23. Sugiyama K, Kaji N, Hiraga K (1998) *Acta Crystall C* 54:445
24. Zhang Z, Kuo KH (1987) *J. Microscopy* 146:313
25. Zhou DS, Ye HQ, Li DX, Kuo KH (1988) *Phys Rev Lett* 60:2180
26. Zhang H, Wang DH, Kuo KH (1988) *Phys Rev B* 37:6220
27. Wang N, Chen H, Kuo KH (1987) *Phys Rev Lett* 59:1010
28. Wang N, Kuo KH (1989) *Phil Mag* 60:347
29. Donnay G, Donnay DH, Iijima S (1977) *Acta Crystall* A33:622
30. Koch E (1999) *International tables for crystallography*, 2nd edn. Kluwer, Dordrecht, V. C, Sect 1.3, p 10